Surface morphology of [11$\bar{2}$0] *a*-plane GaN growth by MOCVD on [1$\bar{1}$02] *r*-plane sapphire*

Xu Shengrui(许晟瑞)†, Hao Yue(郝跃), Duan Huantao(段焕涛), Zhang Jincheng(张进城), Zhang Jinfeng(张金凤), Zhou Xiaowei(周晓伟), Li Zhiming(李志明), and Ni Jinyu(倪金玉)

(Key Laboratory of Wide Band-Gap Semiconductor Materials and Devices, School of Microelectronics, Xi dian University, Xi'an 710071, China)

Abstract: Nonpolar *a*-plane [11$\bar{2}$0] GaN has been grown on *r*-plane [1$\bar{1}$02] sapphire by MOCVD, and investigated by high resolution X-ray diffraction and atomic force microscopy. As opposed to the *c*-direction, this particular orientation is non-polar, and it avoids polarization charge, the associated screening charge and the consequent band bending. Both low-temperature GaN buffer and high-temperature AlN buffer are used for *a*-plane GaN growth on *r*-plane sapphire, and the triangular pits and pleat morphology come forth with different buffers, the possible reasons for which are discussed. The triangular and pleat direction are also investigated. A novel modulate buffer is used for *a*-plane GaN growth on *r*-plane sapphire, and with this technique, the crystal quality has been greatly improved.

Key words: GaN; AFM; HRXRD; *a*-plane

DOI: 10.1088/1674-4926/30/4/043003 **PACC:** 7280; 6855

1. Introduction

GaN-based semiconductors and their heterostructures have recently attracted considerable interest due to their potential for visible or ultraviolet light-emitting diodes (LEDs), laser diodes (LDs) and high-power transistors grown on either *c*-plane sapphire or SiC[1, 2]. Epitaxy toward the *c* orientation leads to undesirable spontaneous and piezoelectric polarization effects, which would result in inclined bands and significantly reduce the carrier recombination rate in quantum wells grown on such polar substrates. Although the electric field can be advantageous for two-dimensional electron gas formation in FETs without external doping, it causes spatial separation of electrons and holes in quantum wells of light emitting diode (LED), such a separation resulting in a low internal quantum efficiency of the emitting devices. It also causes a red shift in LEDs and makes the emission wavelength dependent on injection unless very thin quantum wells are employed[3, 4]. One approach to overcome this problem is to grow *m*-plane or *a*-plane hexagonal GaN that is not polar. However, extended defect densities in non-polar *a*-plane [11$\bar{2}$0] GaN are very high. *a*-plane GaN on *r*-plane Al_2O_3 have a TD density of 3×10^{10} cm^{-2} and a basal stacking fault density of 3.5×10^5 cm^{-1}[5, 6]. The crystalline quality of *a*-plane GaN is very poor[7, 8]. In this paper, the possible reasons for striped features and surface undulations of *a*-plane GaN with different buffers are discussed, and the triangular and pleat direction are also investigated.

2. Experiment

[11$\bar{2}$0] *a*-plane GaN films were grown on [1$\bar{1}$02] *r*-plane sapphire by MOCVD. After chemical cleaning, sapphire substrates, one at a time, were loaded into the low-pressure custom-designed MOCVD system. We used high-temperature AlN and low-temperature GaN as buffer layers. The growth temperature and thickness of the low-temperature buffer layer were 550 °C and 25 nm, while the growth temperature and thickness of the high-temperature buffer layer were 1020 °C and around 50 nm. A novel combine of low-temperature AlN, high-temperature with pulse AlN and high-temperature AlGaN buffer layer was also used, and the temperature and the thickness of the three parts were 550, 1050, 1020 °C and 25, 50, 50 nm, respectively. After buffer layer growth, the temperature was raised to the value between 1000 and 1020 °C, and the *a*-plane epilayer of approximately 1.5 μm thick GaN films was grown subsequently. The new structure is shown in Fig. 1. Trimethylgallium (TMGa), trimethylaluminum (TMAl) and ammonia were used as the Ga, Al and N sources, respectively. The as grown samples were characterized by atomic force microscopy (AFM) and high-resolution X-ray diffraction.

3. Results and discussion

The [11$\bar{2}$0] *a*-plane GaN films were grown on [1$\bar{1}$02] *r*-plane sapphire but the [0001] *c*-plane GaN films were grown on [0001] *c*-plane sapphire, so their morphology and crystal quality show great difference. The epitaxial relationships of the *r*-plane sapphire substrate and atoms array are shown in Fig. 2.

With different buffer layers, the *a*-plane GaN shows different surface morphologies. Figure 3(a) shows the effect of low temperature GaN buffer on *a*-GaN surface morphology

* Project supported by the National Natural Science Foundation of China (No. 60736033) and the State Key Development Program for Basic Research of China (No. 513270407).

† Corresponding author. Email:shengruixidian@126.com

Received 8 September 2008, revised manuscript received 19 November 2008

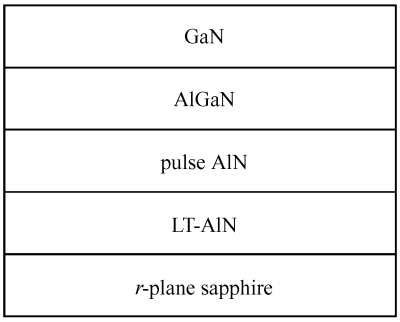

Fig. 1. Schematic representations of the new structure.

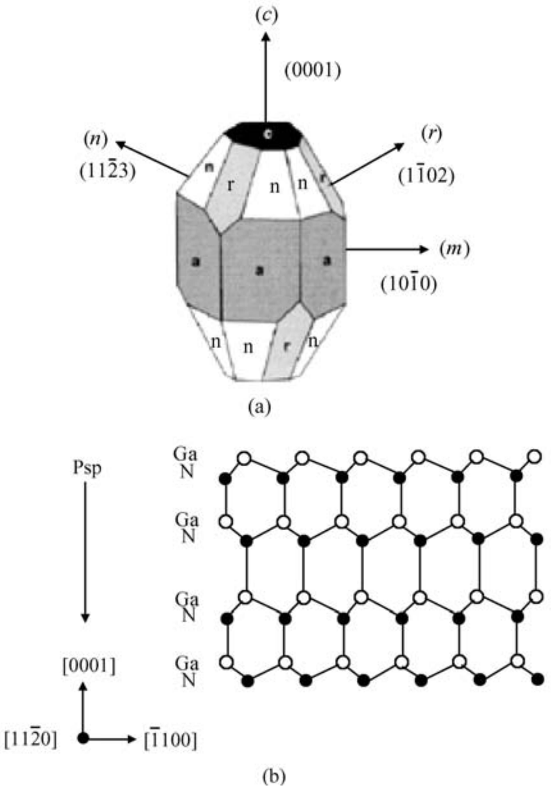

Fig. 2. Schematic representations of (a) the epitaxial relationship between the *r*-plane sapphire substrate of the *a*-plane GaN film and (b) the plan view of the surface atoms which lie on the *a*-plane GaN surface.

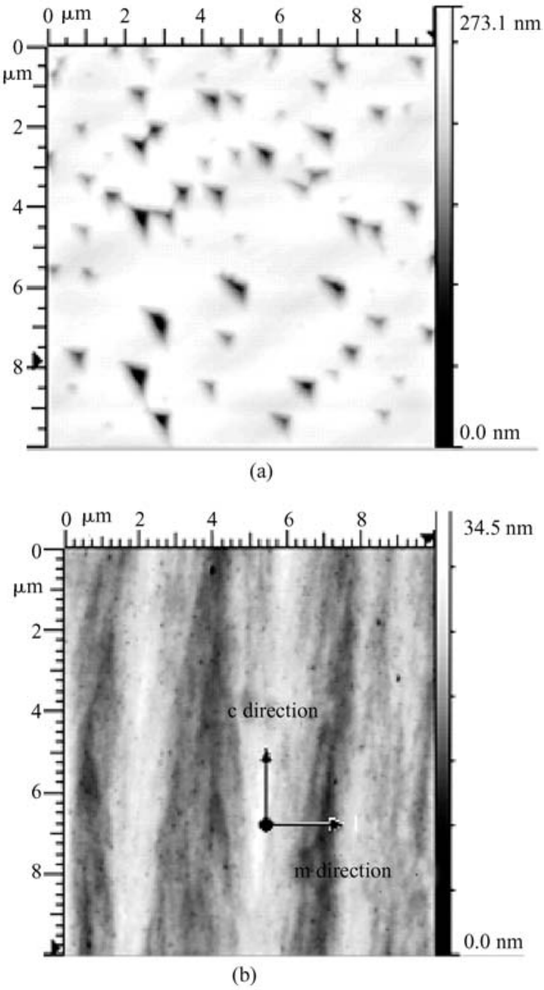

Fig. 3. Surface morphology of AFM for *a*-plane GaN (a) with the low-temperature GaN buffer layer and (b) with the high-temperature AlN buffer layer.

that is examined by AFM. Although with different-sized pits on the surface, they have the same orientation of every triangle side. Figure 3(b) shows the effect of high-temperature AlN on *a*-plane GaN surface morphology that is examined by AFM. From this image, the *a*-plane GaN shows stripe features along the *c*-direction, and surface undulation along the *m*-direction $[1\bar{1}00]$ as well, which is perpendicular to the *c*-direction [0001].

From the elongated stripe growth, we can also conclude that the growth rate along the *c*-direction is much higher than that along the *m* direction. The ratio of the lateral growth rate along the *c*-direction to the vertical growth rate was around 3–4[10–12], which further proves our explanation. The surface undulate of *a*-plane GaN on the low-temperature GaN buffer layer is 273.1 nm, and that of the high-temperature AlN buffer layer *a*-plane GaN is 34.5 nm. The root mean square (RMS) of the low-temperature GaN buffer layer $10\times10\,\mu m^2$ *a*-plane GaN is 22.4 nm, and that of the high-temperature AlN buffer layer $10\times10\,\mu m^2$ *a*-plane GaN is 3.45 nm. Figure 4(a) shows the cross-sectional of AFM with the low-temperature GaN as buffer layer, and Figure 4(b) shows the cross-sectional of AFM with the high-temperature AlN as buffer layer. The GaN with high-temperature AlN buffer layer shows great pleat morphology, and the GaN with low-temperature buffer layer shows many smallness triangle pits. The 3D view of AFM for *a*-plane GaN with different buffer layers is shown in Fig. 5.

Surface morphology measurements of *a*-plane GaN with $1\times1\,\mu m^2$ AFM is employed to determine the direction of the triangular pit. On the basis of the benchmark side of the sapphire, we determine the direction of triangular pit. Its hypotenuse is along the *m*-direction and the perpendicularity line of the hypotenuse is along the *c*-direction. The symmetry side face of the triangular pit is two inclined $[10\bar{1}1]$ facets. Associate with the defects, which are characteristically observed under *c*-plane GaN. For a *c*-plane film, the V defect is an open, inverted pyramid which is bound by the pyramidal $[10\bar{1}1]$ facets commonly encountered in GaN MOCVD growth[13, 14]. Due to the nonpolar orientation, the V defect appears in the GaN film on its side, as shown schematically in Fig. 6(b). AlN film grown at low temperature promotes a 3D growth

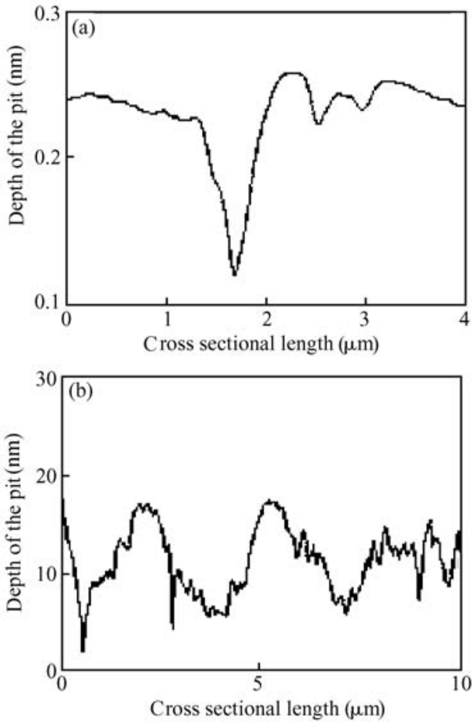

Fig. 4. Cross-sectional of AFM for *a*-plane GaN with (a) the low-temperature GaN as buffer layer and (b) the high-temperature AlN as buffer layer.

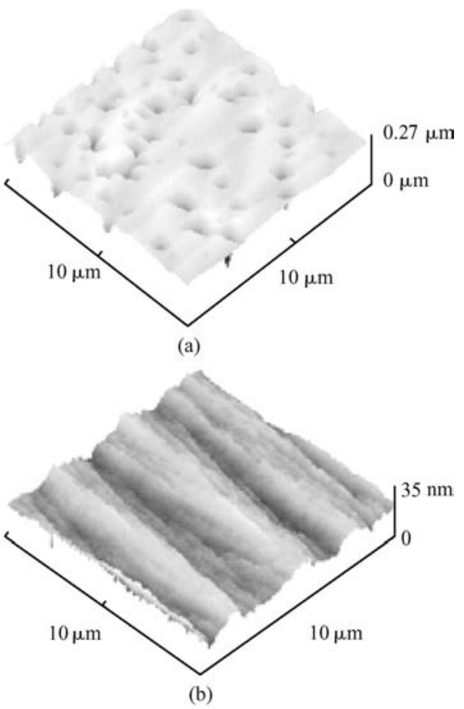

Fig. 5. 3D view of AFM for *a*-plane GaN with (a) the low-temperature GaN as buffer layer and (b) the high-temperature AlN as buffer layer.

mode, producing large islands with discrete $(10\bar{1}1)$, $(01\bar{1}1)$, and $(000\bar{1})$ side facets, and their coalescence is incomplete under these conditions and is a consequence of the $(000\bar{1})$ plane being of a different crystallographic family from the $(10\bar{1}1)$ and $(01\bar{1}1)$[15].

These pits form upon island growth and coalescence at the early stages of high temperature growth. Since the pits do not close up throughout the course of the high temperature growth, the pit facets are extremely stable and slow growing.

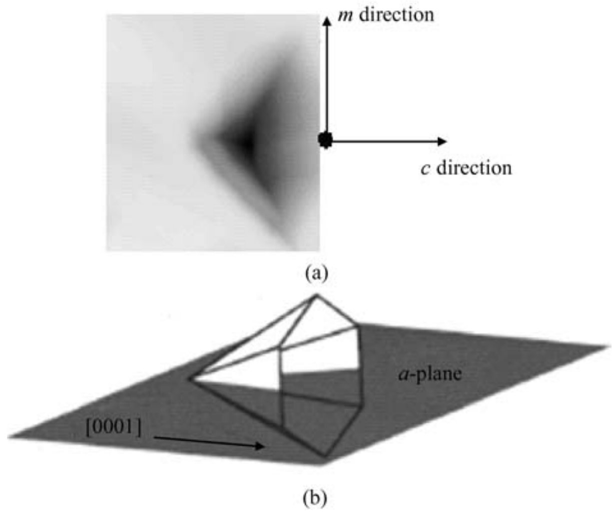

Fig. 6. (a) Surface morphology measurements of *a*-plane GaN with 1×1 μm^2 AFM; (b) V defect, shown schematically, which is commonly observed in *c*-plane growth.

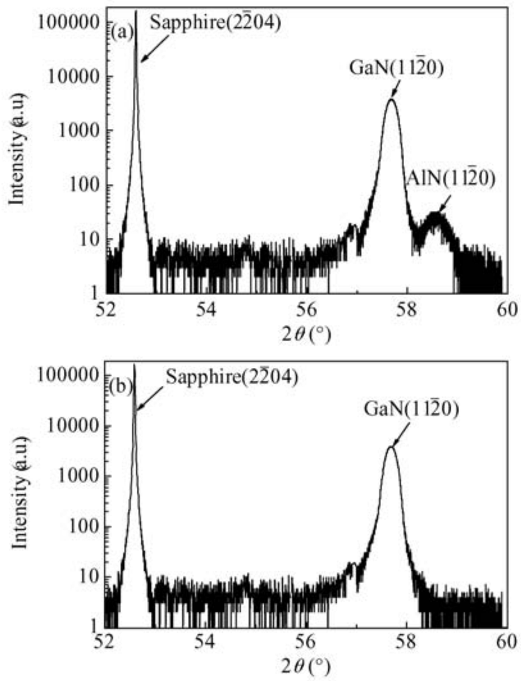

Fig. 7. XRD spectra using 2θ–ω scan for (a) *a*-plane GaN grown with HT AlN buffer layer on *r*-plane $[1\bar{1}02]$ sapphire and (b) *a*-plane GaN grown with LT GaN buffer layer on *r*-plane $[1\bar{1}02]$ sapphire.

Structural characteristics of the as-grown *a*-plane GaN films were evaluated by HRXRD. As shown in Fig. 7, the 2θ–ω scans of the as-grown HT AlN buffer layer sample exhibit two peaks that are assigned to the diffractions from the $[11\bar{2}0]$ of *a*-plane AlN buffer, and from the $[11\bar{2}0]$ of *a*-plane GaN. No other diffraction from GaN is observed within the detection limits of this technique. All these indicate that the GaN films are uniquely $[11\bar{2}0]$ *a*-plane oriented as the *a*-plane GaN films grown by MOCVD with the HT-AlN or LT-GaN buffer layer. The full width at half maximum (FWHM) values of X-ray 2θ–ω scan curve are 0.2072° and 0.2396° for samples grown on LT-GaN and HT-AlN buffer layers, respectively. The *a*-plane GaN on LT-GaN buffer layer has an improved crystalline

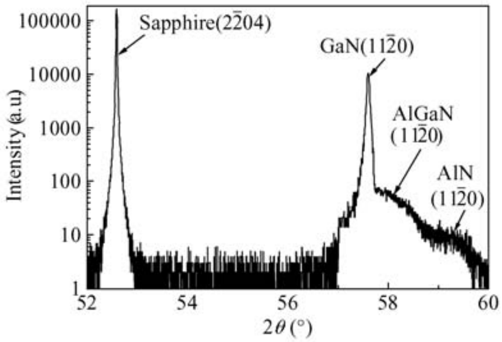

Fig. 8. XRD spectra using 2θ–ω scan for modulate buffer.

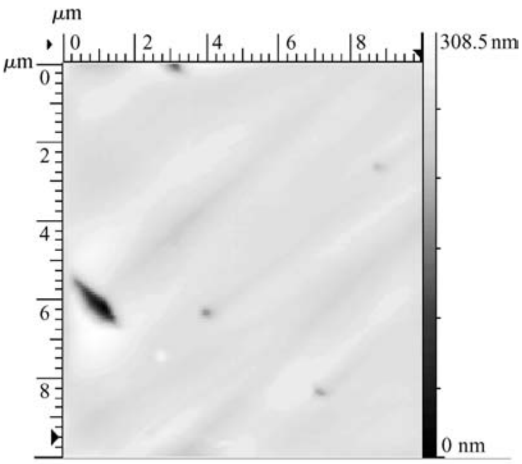

Fig. 9. Surface morphology of AFM for modulate buffer.

quality, but its RMS is much larger. Therefore, the choice of optimum buffer layer should be a compromise of crystalline quality and the surface morphology.

When grown on modulate buffer structure, the quality of the material is significantly improved. The FWHM value of X-ray 2θ–ω scan curve is 0.1626°, and the number of triangle pits decreases significantly. The density of the triangle pits is from 5.6×10^7 to 5×10^6 cm^{-2}. The XRD spectra and the surface morphology of AFM for modulate buffer are shown in Figs. 8 and 9 respectively. The idea of the new structure is forming a grads buffer to decrease the poor mismatch with the substrate of nearly 10%. This structure should be effective to improve the quality of nonpolar GaN material.

4. Conclusions

Eliminating polarization-related electric fields and reducing extended defect densities are essential for improving III-nitride film growth and device performance. *A*-plane GaN growth by MOCVD with high-temperature AlN, low-temperature GaN as buffer layer was studied. The *a*-plane GaN shows different surface morphology: with high-temperature AlN, the *a*-plane GaN shows stripe features along the *c*-direction, and surface undulation along the *m*-direction $[1\bar{1}00]$. In the other case, the hypotenuse of the triangular pit is along the *m* direction and the perpendicularity line of the hypotenuse is along the *c* direction. A novel modulate buffer is used for *a*-plane GaN growth on *r*-plane sapphire. The density of the triangle pits is from 5.6×10^{-7} to 1.65×10^{-7} cm^{-2}. This method reduces crystal lattice mismatch of the GaN to the AlN buffer, and the surface morphology and quality of the material show significant improvement. We will pay more attention to improving the crystalline quality in future study.

References

[1] Xing H, Keller M D S, Mates T, et al. Nonpolar *a*-plane p-type GaN and p-n junction diodes. J Appl Phys, 2008, 101(8): 4494

[2] Palacios T, Shen L, Keller S, et al. Nitride-based high electron mobility transistors with a GaN spacer. Appl Phys Lett, 2006, 89: 073508

[3] Bastek B, Bertram F, Christen J, et al. *A*-plane GaN epitaxial lateral overgrowth structures: growth domains, morphological defects, and impurity incorporation directly imaged by cathodoluminescence microscopy. Appl Phys Lett, 2008, 92: 212111

[4] Zhu T, Martin D, Butte R, et al. *A*-plane GaN grown on r-plane sapphire substrates by hydride vapor phase epitaxy. J Cryst Growth, 2007, 300: 186

[5] Yan J F, Guo L W, Zhang J, et al. Characteristics of the improved *a*-plane GaN films grown on *r*-plane sapphire with two-step AlN buffer layer. J Cryst Growth, 2007, 307: 35

[6] Ni X, Fu Y, Moon Y T, et al. Optimization of $[11\bar{2}0]$ *a*-plane GaN growth by MOCVD on $[1\bar{1}02]$ *r*-plane sapphire. J Cryst Growth, 2006, 290: 166

[7] Langer R, Simon J, Ortiz V, et al. Giant electric fields in unstrained GaN single quantum wells. Appl Phys Lett, 1999, 74: 3827

[8] Craven M D, Lim S H, Wu F, et al. Threading dislocation reduction via laterally overgrown nonpolar $[11\bar{2}0]$ *a*-plane GaN. Appl Phys Lett, 2002, 81: 1201

[9] Imer B, Wu F, Speck J S, et al. Growth evolution in sidewall lateral epitaxial overgrowth (SLEO). J Cryst Growth, 2007, 306: 330

[10] Ko T S, Wang T C, Gao R C, et al. Study on optimal growth conditions of *a*-plane GaN grown on *r*-plane sapphire by metal-organic chemical vapor deposition. J Cryst Growth, 2007, 300: 308

[11] Ni X, Özgür Ü, Morkoc H, et al. Epitaxial lateral overgrowth of *a*-plane GaN by metalorganic chemical vapor deposition. J Appl Phys, 2007, 102: 053506

[12] Darakchieva V, Paskova T, Schubert M. Effect of anisotropic strain on phonons in *a*-plane and *c*-plane GaN layers. J Cryst Growth, 2007, 300: 233

[13] Wu F, Craven M D, Lim S H, et al. Polarity determination of *a*-plane GaN on *r*-plane sapphire and its effects on lateral overgrowth and heteroepitaxy. J Appl Phys, 2003, 94: 166

[14] Li D S, Chen H, Yu H B, et al. Effects of reactor pressure on GaN-based light-emitting diodes grown on *a*-plane sapphire substrates. J Cryst Growth, 2004, 263: 76

[15] Hollander J L, Kappers M J, McAleese C, et al. Improvements in *a*-plane GaN crystal quality by a two-step growth process. Appl Phys Lett, 2008, 92: 101104

[16] Craven M D, Lim S H, Wu F, et al. Structural characterization of nonpolar $(11\bar{2}0)$ *a*-plane GaN thin films grown on $(1\bar{1}02)$ *r*-plane sapphire. Appl Phys Lett, 2002, 81: 469